Divide-Then-Rule: A Cluster-Driven Hierarchical Interpolator for Attribute-Missing Graphs

Yaowen Hu
College of Computer Science and Technology, National University of Defense Technology
Changsha, China

Wenxuan Tu
School of Computer Science and Technology, Hainan University
Haikou, China

Yue Liu
College of Computer Science and Technology, National University of Defense Technology
Changsha, China

Miaomiao Li
Changsha University
Changsha, China

Wenpeng Lu
Key Laboratory of Computing Power Network and Information Security, Ministry of Education, Shandong Computer Science Center (National Supercomputer Center in Jinan), Qilu University of Technology (Shandong Academy of Sciences)
Jinan, China

Zhigang Luo
Xiangjiang Laboratory
Changsha, China

Xinwang Liu†
College of Computer Science and Technology, National University of Defense Technology
Changsha, China

Ping Chen
School of Information and Communication Engineering, North University of China
Taiyuan, China

arXiv:2507.10595v1 [cs.LG] 12 Jul 2025

Abstract

Deep graph clustering (DGC) for attribute-missing graphs is an unsupervised task aimed at partitioning nodes with incomplete attributes into distinct clusters. Addressing this challenging issue is vital for practical applications. However, research in this area remains underexplored. Existing imputation methods for attribute-missing graphs often fail to account for the varying amounts of information available across node neighborhoods, leading to unreliable results, especially for nodes with insufficient known neighborhood. To address this issue, we propose a novel method named Divide-Then-Rule Graph Completion (DTRGC). This method first addresses nodes with sufficient known neighborhood information and treats the imputed results as new knowledge to iteratively impute more challenging nodes, while leveraging clustering information to correct imputation errors. Specifically, Dynamic Cluster-Aware Feature Propagation (DCFP) initializes missing node attributes by adjusting propagation weights based on the clustering structure. Subsequently, Hierarchical Neighborhood-aware Imputation (HNAI) categorizes attribute-missing nodes into three groups based on the completeness of their neighborhood attributes. The imputation is performed hierarchically, prioritizing the groups with nodes that have the most available neighborhood information. The cluster structure is then used to refine the imputation and correct potential errors. Finally, Hop-wise Representation Enhancement (HRE) integrates information across multiple hops, thereby enriching the expressiveness of node representations. Experimental results on six widely used graph datasets show that DTRGC significantly improves the clustering performance of various DGC methods under attribute-missing graphs.

CCS Concepts

• **Computing methodologies** → *Machine learning algorithms.*

Keywords

Deep Graph Clustering, Attribute-Missing Graph, Graph Completion, Hierarchical

1 Introduction

Deep Graph Clustering (DGC) [18, 25, 55] is a fundamental task in unsupervised learning that aims to cluster nodes based on graph structures, grouping similar nodes together without reliance on labels. In recent years, DGC methods have achieved notable success in various practical applications, including community detection, recommendation systems, and facial recognition [21, 36, 40, 49]. Existing DGC approaches typically rely on contrastive learning [31, 50, 52] or reconstruction models [3, 10, 12]. These methods either maximize the similarity between nodes in the same cluster or reconstruct node features to enhance clustering effectiveness.

Existing DGC methods operate under a crucial assumption that the attributes of all nodes are complete and reliable [16, 41, 51]. However, in real-world scenarios, issues like privacy protection and copyright restrictions during data collection often lead to incomplete node attributes. Attribute-missing graphs typically manifest in two patterns: (1) Uniform missing, where some attributes of each node are partially missing[6, 57]; and (2) Structural missing, where all attributes of certain nodes are entirely missing[3, 8, 47]. This paper focuses particularly on the latter, as it is more common and challenging in practical applications. For instance, in e-commerce,

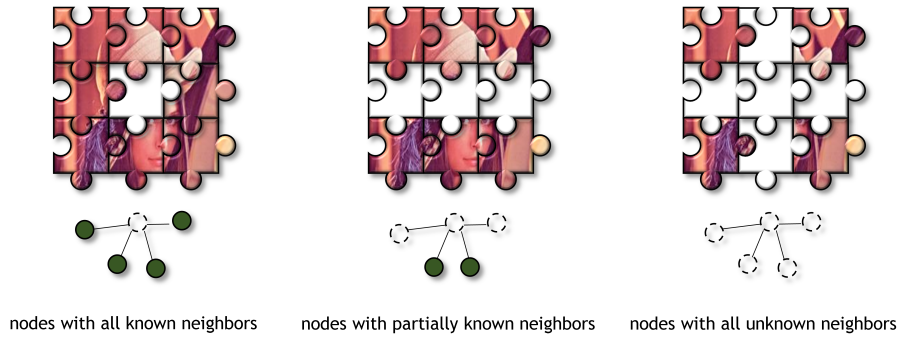

Figure 1: Illustration of the hierarchical differentiation of nodes based on the completeness of their neighborhood attributes. The figure employs different jigsaw puzzle states to represent three categories of nodes: "nodes with all known neighbors" are akin to well-defined edge pieces of a jigsaw puzzle, which can be easily reconstructed; "nodes with partially known neighbors" correspond to jigsaw puzzle regions that are partially assembled, requiring additional information from neighboring pieces to complete; and "nodes with all unknown neighbors" resemble blank sections lacking sufficient contextual information.

users may choose not to provide feedback on specific products due to privacy concerns. Although considerable attention has been devoted to imputing attribute-missing graphs[3, 28, 44], most of these studies encounter significant challenges in clustering tasks: (1) Semi-supervised imputation methods rely heavily on partial label information and cannot be directly applied to clustering. For example, label propagation (LP) [39, 48] propagates known labels to unlabeled nodes via neighboring nodes, making it unsuitable for fully unsupervised clustering tasks. (2) Plug-and-play imputation methods often lack a mechanism to account for clustering structures. For instance, feature propagation (FP) [1, 20, 24] propagates features across edges between nodes without regard to cluster membership, maintaining the same message-passing (MP) intensity regardless of whether two nodes belong to the same cluster.

Although the aforementioned methods improve clustering performance on attribute-missing graphs through imputation, they share a critical limitation: **These methods fail to account for differences in neighborhood information, relying on a uniform imputation strategy that leads to unreliable results for nodes with insufficient known information.** For example, when "nodes with all unknown neighbors" are interconnected, the imputation results for the internal missing nodes become unreliable. Existing approaches typically propagate information indiscriminately from distant attribute-complete nodes, causing the imputed node attributes to deviate from their original characteristics. Consequently, these nodes become difficult to cluster accurately. To overcome these limitations, we draw inspiration from the principle of Prägnanz in Gestalt psychology [34, 43]. Specifically, when humans encounter an incomplete scene, they tend to prioritize known and high-confidence information, using it to progressively infer the unknown. As illustrated in Fig. 1, an attribute-missing graph can be analogized to a partially disassembled jigsaw puzzle: while the adjacency relations between pieces (i.e., the graph structure) remain intact, the patterns on some pieces (i.e., node attributes) are missing. To restore the puzzle, one typically using these easily recognizable parts to infer the missing ones step by step.

Based on these observations, there is an urgent need for a graph imputation scheme that supports hierarchical processing and is tailored to different types of attribute-missing nodes. To address this, we propose a novel approach, termed **D**ivide-**T**hen-**R**ule **G**raph **C**ompletion (DTRGC). The core idea of DTRGC is to iteratively impute nodes, starting with those having sufficient known neighborhood information, while using the imputed results as new knowledge and leveraging clustering information correct imputation errors. DTRGC consists of three main steps: First, Dynamic Cluster-aware Feature Propagation (DCFP) initializes missing node attributes and adjusts propagation weights based on the clustering structure. This enhances feature transmission among intra-cluster nodes and reduces interference from heterogeneous nodes. Next, Hierarchical Neighborhood-aware Imputation (HNAI) categorizes nodes into three types based on attribute completeness within their neighborhoods. It applies distinct imputation strategies to refine the imputation process. Finally, Hop-wise Representation Enhancement (HRE) enriches node representations by gradually expanding the neighborhood scope and integrating multi-hop information.

The main contributions of our work are as follows:

- This paper presents DTRGC, the first framework tailored for clustering on attribute-missing graphs via hierarchical processing, in which nodes are classified based on the completeness of their neighborhood attributes and are imputed using category-specific strategies.
- Three core components are developed within DTRGC: DCFP, HNAI, and HRE. These modules operate synergistically, progressively imputing missing node attributes and ensuring that each node category receives appropriate treatment, thus enhancing overall imputation quality.
- Experimental evaluations on six widely used graph datasets show that DTRGC improves the clustering performance of all tested DGC methods on the attribute-missing graphs. Notably, in non-deep clustering settings, the attribute-missing graphs imputed by DTRGC even outperform their attribute-complete counterparts.

2 Relates Work

2.1 Attribute-complete Deep Graph Clustering

In recent years, DGC has made significant advancements in handling attribute-complete graphs. Existing methods are broadly classified into two categories: (1) Graph Autoencoder-based Methods.

These methods encode node features into low-dimensional representations and utilize decoders to reconstruct the original features from the learned embeddings [19, 27, 30, 31, 35, 46]. For instance, the Embedding Graph AutoEncoder (EGAE) integrates k-means clustering with autoencoder training [54]. This integration enhances the consistency between node representations and clustering. (2) Contrastive Learning-based Methods. These methods optimize node embeddings by creating positive and negative sample pairs, aiming to pull positive samples closer while pushing negative samples apart in the embedding space [14, 29, 38, 45]. The Simple Contrastive Graph Clustering (SCGC) improves clustering efficiency through simplified data augmentation and a streamlined architecture [15]. Similarly, Peng et al. [22] introduced the Dual Contrastive Learning Network (DCLN), which incorporates dual mechanisms to prevent feature collapse and enhance the discriminative power of node embeddings. Despite their significant achievements in clustering attribute-complete graphs, these methods generally rely on the assumption of complete and reliable node attributes.

2.2 Attribute-missing Graph Imputation

The objective of attribute-missing graph imputation is to enable effective learning when node attributes are partially or entirely absent. Existing approaches can be broadly categorized into two classes. (1) GCN-variant Models, directly operate on attribute-incomplete graphs and recover missing features during training. These methods typically extend Graph Convolutional Networks (GCNs) [2, 11, 13, 37] to handle incomplete attributes. For example, the Structural Attribute Transformer (SAT) [3] models the joint distribution of graph structure and node features via distributional learning. GCNMF [26] integrates a Gaussian mixture model to address missing features, while PaGNN [7] proposes a partial message-passing scheme using only available attributes. Although effective in semi-supervised settings, these methods rely on label, limiting their applicability in unsupervised tasks such as graph clustering. (2) Feature Imputation Methods, reconstructs missing attributes prior to learning, without relying on parameterized encoders or training.[9, 42, 52] A classical method is label propagation (LP) [17, 39], which infers unknown labels by diffusing known ones, but it requires label and is unsuitable for clustering. To overcome this limitation, recent methods such as Feature Propagation (FP) [24, 53] and Pseudo-Confidence Feature Imputation (PCFI) [32] leverage graph topology to recover missing features. FP performs feature diffusion, while PCFI assigns confidence scores to each imputed feature. However, these methods typically adopt a uniform imputation strategy, overlooking variations in neighborhood completeness, which can lead to unreliable imputations for nodes with sparse known neighbors and thus degrade clustering performance.

3 Method

3.1 Notations and Problem Definition

Notations. *Let $\mathcal{G} = \{\mathcal{V}, \mathcal{E}, \mathbf{H}\}$ denote an undirected graph, where $\mathcal{V} = \{v_n\}_{n=1}^{N}$ is the vertex set with N nodes, $\mathcal{E}$ is the edge set, $\mathbf{H} \in \mathbb{R}^{N\times d}$ is the node attribute matrix where d denotes the feature dimension of node.* $\mathbf{A}$ *is the adjacency matrix representing the relationships between nodes. Specifically, $a_{ij} = 1$ if there is an edge between nodes v_i and v_j, and $a_{ij} = 0$ otherwise.*

Definition 1. **(Attribute-Missing Graph)** *The attribute-missing graph refers to a graph in which certain nodes lack attributes entirely, meaning that some nodes have no associated feature representations. Thus, the nodes set $\mathcal{V}$ of the graph can be divided into two subsets: the attribute-complete nodes $\mathcal{V}^c = \{v_n^c\}_{n=1}^{N^c}$ and the attribute-missing nodes $\mathcal{V}^m = \{v_n^m\}_{n=1}^{N^m}$. Accordingly, $\mathcal{V} = \mathcal{V}^c \cup \mathcal{V}^m, \mathcal{V}^c \cap \mathcal{V}^m = \emptyset$ and $N = N^c + N^m$. Based on these notations, an attribute-missing graph can be formulated as $\widetilde{\mathcal{G}} = \{\mathcal{V}^m, \mathcal{E}\}$.*

Definition 2. **(Attribute-Missing Graph Clustering)***Given an unlabeled attribute-missing graph $\widetilde{\mathcal{G}} = \{\mathcal{V}^m, \mathcal{E}\}$ with K clusters, the objective is to impute cluster-compatible features for the attribute-missing nodes. Subsequently, DGC is applied to the imputed attribute-missing graph to ensure that similar nodes are grouped into the same cluster.*

3.2 Divide-Then-Rule Graph Completion

As previously discussed, existing methods often fail to account for the varying amounts of available information across node neighborhoods, leading to unreliable results, especially for nodes with insufficient known neighborhood. To realize this approach, we develop the DTRGC framework, which comprises three core components: DCFP, HNAI, and HRE. The working mechanisms of these components are detailed in this section, with implementation specifics provided in Algorithm 1.

3.2.1 Dynamic Cluster-aware Feature Propagation. DCFP constitutes the first step of DTRGC, designed to initialize missing attributes in the graph by leveraging the structural clusters of nodes. Unlike standard feature propagation, which uniformly propagates information across the entire graph, DCFP dynamically adjusts the propagation intensity based on whether nodes belong to the same cluster, thereby reinforcing feature propagation within clusters while suppressing feature diffusion across clusters.

In each iteration, node features are propagated according to the normalized adjacency matrix, followed by a backtracking step to ensure that attribute-complete nodes remain unchanged.

$$\begin{aligned} \mathbf{H}^{(t+1)} &= \hat{\mathbf{A}}\mathbf{H}^{(t)}, \\ \mathbf{H}_c^{(t+1)} &= \mathbf{H}_c^{(t)} = \mathbf{H}_c^{(0)}. \end{aligned} \tag{1}$$

To leverage cluster structural information effectively, DCFP performs classic k-means clustering after every T iteration and subsequently adjusts the adjacency matrix to reflect the updated cluster structure. Specific adjustment as follows:

$$\hat{a}_{ij}^{(t+1)} = \begin{cases} \alpha\hat{a}_{ij}^{(t)}, & \text{if } c_i = c_j \text{ and } t \bmod T = 0 \\ \beta\hat{a}_{ij}^{(t)}, & \text{if } c_i \neq c_j \text{ and } t \bmod T = 0 \\ \hat{a}_{ij}^{(t)}, & \text{otherwise,} \end{cases} \tag{2}$$

where, c_i and c_j represent the clusters to which nodes i and j belong, respectively. Setting $\alpha > 1$ enhances the feature propagation between nodes within the same cluster is enhanced, whereas setting $\beta < 1$ weakens propagation across clusters.

E. Rossi et al. [24] prove the convergence of a similar formula as shown in Eq.(1) and provided the required number of iterations for convergence in discrete time. Based on this result, T at 40 in this work. FP and adjacency matrix adjustments are performed

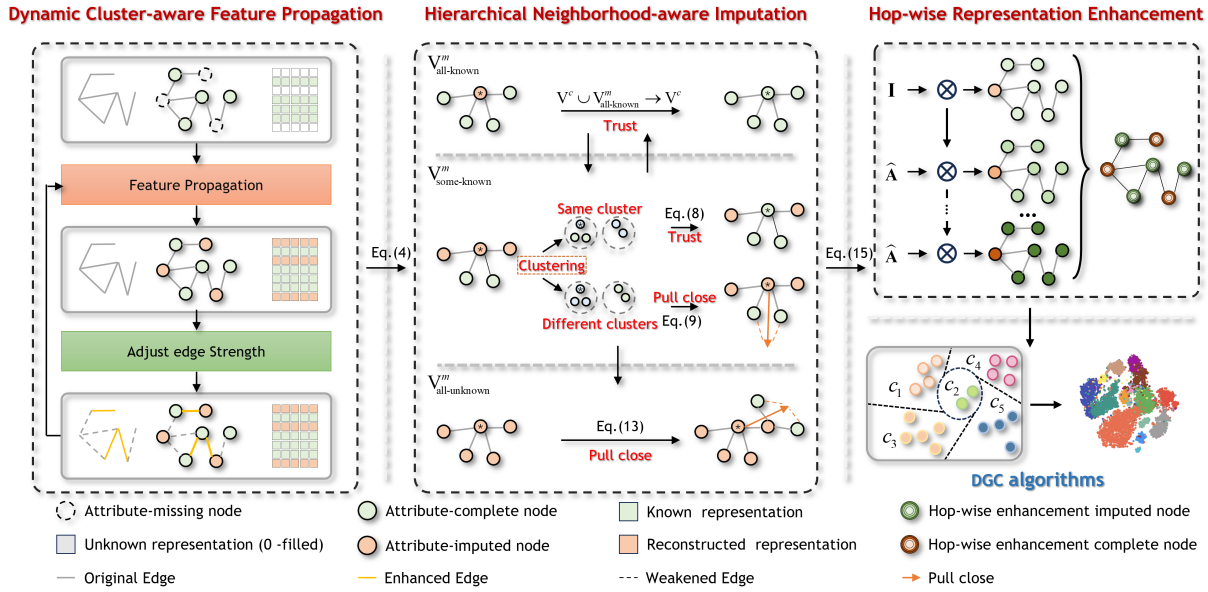

Figure 2: The overall architecture of the DTRGC. In this framework, we first initialize the missing node attributes while adjusting propagation weights based on cluster structures to enhance intra-cluster propagation and suppress inter-cluster propagation. Next, the attribute-missing nodes are categorized into three groups based on the completeness of their neighborhood attributes, and distinct imputation strategies are applied to refine the imputation process for each group. Finally, multi-hop propagation is utilized to extend the neighborhood scope. As a result, the attribute-missing graphs processed by DTRGC can be directly used with any DGC algorithm.

alternately, with the modified adjacency matrix $\hat{\mathbf{A}}_{ij}^{(t)}$ used to update node features over the next T iterations.

3.2.2 Hierarchical Neighborhood-aware Imputation. Although DCFP achieves alternating optimization of clustering and imputation, it overlooks the varying needs of different types of attribute-missing nodes and does not fully utilize the neighborhood structural information for targeted imputation. To address this limitation, we propose the HNAI, which follows a progressive imputation process that prioritizes information-rich nodes, using them as references to impute information-scarce nodes.

Specifically, HNAI classifies attribute-missing nodes into three categories based on the attribute completeness of their 1-hop neighborhood: (1) $\mathcal{V}^m_{\text{all-known}}$, where all neighbors are attribute-complete; (2) $\mathcal{V}^m_{\text{some-known}}$, where some neighbors are attribute-complete and others are attribute-missing; and (3) $\mathcal{V}^m_{\text{all-unknown}}$, where all neighbors are attribute-missing. These categories are illustrated in Fig. 1, and the classification process is formally defined by the following equation:

$$v_i \in \mathcal{V}^m = \begin{cases} \mathcal{V}^m_{\text{all-known}} & \text{if } \forall v_j \in \mathcal{N}(i), v_j \in \mathcal{V}^c \\ \mathcal{V}^m_{\text{some-known}} & \text{if } \exists v_j \in \mathcal{N}(i), v_j \in \mathcal{V}^c \\ \mathcal{V}^m_{\text{all-unknown}} & \text{if } \forall v_j \in \mathcal{N}(i), v_j \in \mathcal{V}^m, \end{cases} \tag{3}$$

where, v_i denotes an attribute-missing node, v_j represents a neighboring node of the attribute-missing node, and $\mathcal{N}(i)$ indicates the 1-hop neighborhoods of node i.

Subsequently, specific imputation strategies are applied to each category of attribute-missing nodes. The iterative process involves: (1) imputing $\mathcal{V}^m_{\text{all-known}}$, (2) imputing $\mathcal{V}^m_{\text{some-known}}$, and (3) reclassification using Eq. (3). Finally, $\mathcal{V}^m_{\text{all-unknown}}$ nodes, the most challenging to impute, are estimated last.

Nodes with All Known Neighbors $\mathcal{V}^m_{\text{all-known}}$. Based on the homogeneity assumption, these neighboring nodes typically belong to the same cluster during the clustering process. Thus, $\mathcal{V}^m_{\text{all-known}}$ can be directly treated as attribute-complete nodes, as justified in **Proposition 1**:

$$\mathcal{V}^c \leftarrow \mathcal{V}^c \cup \mathcal{V}^m_{\text{all-known}}. \tag{4}$$

Proposition 1. *For any $v_i \in \mathcal{V}^m_{\text{all-known}}$, its feature imputation is based on a non-negative linear combination of its fully observed neighbors in the 1-hop neighborhood. Therefore, it is reasonable to treat it as an attribute-complete node.*

Proof. For any $v_i \in \mathcal{V}^m_{\text{all-known}}$, its imputation process entirely depends on the attribute-complete nodes in its 1-hop neighborhood. According to Eq.(1), the imputed features of node can be represented as a non-negative linear combination of its attribute-complete neighbors, normalized by the adjacency matrix. Specifically, for any $v_i \in \mathcal{V}^m_{\text{all-known}}$, the imputed feature $\mathbf{x}_i$ can be written as:

$$\mathbf{x}_i = \sum_{v_j \in \mathcal{N}(i)} \hat{a}_{ij} \mathbf{x}_j, \tag{5}$$

where $\hat{a}_{ij} \in (0, 1)$ and $\sum_{v_j \in \mathcal{N}(i)} \hat{a}_{ij} \leq 1$. Thus, this implies that the imputed node feature $\mathbf{x}_i$ lies within the convex hull defined by

the features of its neighbors, ensuring that it is located within the feature space formed by these neighbors.

In the clustering, distance-based clustering algorithms (e.g., k-means) group points that are closer together into the same cluster. As a result, the imputed node v_i correctly reflects its position within the cluster structure and maintains consistency with its neighbors. Therefore, it is reasonable to treat the nodes in $\mathcal{V}^m_{\text{all-known}}$ as attribute-complete nodes, i.e.:

$$\mathcal{V}^c \leftarrow \mathcal{V}^c \cup \mathcal{V}^m_{\text{all-known}}. \tag{6}$$

□

Nodes with Partially Known Neighbors $\mathcal{V}^m_{\text{some-known}}$. The completion of this category of nodes relies on two sources of information: (1) direct propagation from attribute-complete neighbors within their 1-hop neighborhood; and (2) indirect transmission of information from distant attribute-complete nodes through attribute-missing neighbors. To improve imputation accuracy, we apply the following refinement strategy for this category of nodes:

Intra-cluster Reinforcement Strategy (IRS). When a $\mathcal{V}^m_{\text{some-known}}$ node and all of its attribute-complete neighbors belong to the same cluster, this strongly aligns with the homogeneity assumption for graphs. In such cases, the feature of this node can be considered reliable, as its imputed result can be confidently assigned to the correct cluster for clustering. It is then treated as a attribute-complete node by adding it to the set $\mathcal{V}^c$, as represented below:

$$\begin{aligned} &\mathcal{V}^c \leftarrow \mathcal{V}^c \cup \{v_i\}, \quad \forall v_i \in \mathcal{V}^m_{\text{some-known}} \\ &\text{if } \forall v_j \in \mathcal{N}_{\text{known}}(i), c_i = c_j. \end{aligned} \tag{7}$$

Inter-cluster Correction Strategy (ICS). When a $\mathcal{V}^m_{\text{some-known}}$ node and all attribute-complete neighbors do not belong to the same cluster, this significantly violates the homogeneity assumption for graphs. To mitigate this effect, we update the feature of this node using EMA [5], enabling it to gradually move toward the centroid of the features from attribute-complete neighbors, as described by the following equation:

$$\begin{aligned} &v_i \leftarrow \gamma v_i + (1-\gamma) \cdot \text{mean}(\mathcal{N}_{\text{known}}(i)), \forall v_i \in \mathcal{V}^m_{\text{some-known}} \\ &\text{if } \forall v_j \in \mathcal{N}_{\text{known}}(i), c_i \neq c_j, \end{aligned} \tag{8}$$

where, γ represents the smoothing coefficient for EMA.

It is important to note that the IRS and ICS may trigger a chain reaction within the neighborhood of certain $v_i \in \mathcal{V}^m_{\text{some-known}}$, causing nodes categorized as $\mathcal{V}^m_{\text{some-known}}$ and $\mathcal{V}^m_{\text{all-unknown}}$ within this neighborhood to undergo corresponding state transitions, as demonstrated in **Proposition 2**.

Proposition 2. *When a node $v_i \in \mathcal{V}^m_{\text{some-known}}$ is reclassified as an attribute-complete node (i.e., $v_i \in \mathcal{V}^c$):*

*(I) The neighboring nodes in $\mathcal{V}^m_{\text{some-known}}$ **may** be reclassified as $\mathcal{V}^m_{\text{all-known}}$.*

*(II) The neighboring nodes in $\mathcal{V}^m_{\text{all-unknown}}$ **will certainly** be reclassified as $\mathcal{V}^m_{\text{some-known}}$.*

Proof. Consider a node $v_i \in \mathcal{V}^m_{\text{some-known}}$ to which either the IRS or the ICS has been applied. According to these strategies, if certain conditions are met, v_i will be reclassified as an attribute-complete node and added to the $\mathcal{V}^c$:

$$\mathcal{V}^c \leftarrow \mathcal{V}^c \cup \{v_i\}. \tag{9}$$

Effect on Neighboring $\mathcal{V}^m_{\text{some-known}}$ Nodes. Let v_j be a neighbor of v_i, where $v_j \in \mathcal{V}^m_{\text{some-known}}$. After v_i is updated to an attribute-complete node ($v_i \in \mathcal{V}^c$), we consider the impact on v_j:

- **Case 1:** v_i was the only attribute-missing neighbor of v_j. In this case, all neighbors of v_j are now attribute-complete nodes:
$$\forall v_k \in \mathcal{N}(v_j), \quad v_k \in \mathcal{V}^c. \tag{10}$$
According to Eq.(3), v_j is then reclassified as $\mathcal{V}^m_{\text{all-known}}$.
- **Case 2:** v_j has other attribute-missing neighbors in addition to v_i.
Here, v_j will still have both attribute-complete and attribute-missing neighbors, and thus will remain in $\mathcal{V}^m_{\text{some-known}}$.

Effect on Neighboring $\mathcal{V}^m_{\text{all-unknown}}$ Nodes. Consider a neighboring node $v_j \in \mathcal{N}(v_i)$, where initially $v_j \in \mathcal{V}^m_{\text{all-unknown}}$. After v_i is reclassified as an attribute-complete node (i.e., $v_i \in \mathcal{V}^c$), v_j will gain at least one attribute-complete neighbor, specifically v_i:

$$\exists v_i \in \mathcal{N}(v_j), \quad v_i \in \mathcal{V}^c. \tag{11}$$

In this scenario, v_j no longer meets the definition of being in $\mathcal{V}^m_{\text{all-unknown}}$, as it now has an attribute-complete neighbor. Therefore, v_j is reclassified as a node in $\mathcal{V}^m_{\text{some-known}}$.

□

Nodes with All Unknown Neighbors $\mathcal{V}^m_{\text{all-unknown}}$. As analyzed in **Proposition 2**, a significant proportion of nodes initially classified as $\mathcal{V}^m_{\text{all-unknown}}$ are eventually reclassified as $\mathcal{V}^m_{\text{some-known}}$. This result is also quantitatively reflected in Section 4.2. For the remaining $\mathcal{V}^m_{\text{all-unknown}}$ nodes, their imputation is derived entirely from neighbors that are themselves attribute-missing. Referring to the aforementioned ICS, if a node $v_i \in \mathcal{V}^m_{\text{all-unknown}}$ has neighbors in $\mathcal{N}_{\text{some-known}}(i)$ that do not belong to the same cluster, EMA is employed to iteratively adjust the feature of v_i, driving it towards the centroid of its $\mathcal{V}^m_{\text{some-known}}$ neighbors:

$$\begin{aligned} &v_i \leftarrow \gamma v_i + (1-\gamma) \cdot \text{mean}(\mathcal{N}_{\text{some-known}}(i)), \forall v_i \in \mathcal{V}^m_{\text{all-unknown}} \\ &\text{if } \forall v_j \in \mathcal{N}_{\text{some-known}}(i), c_i \neq c_j, \end{aligned} \tag{12}$$

where, $\text{mean}(\mathcal{N}_{\text{some-known}}(i))$ denotes the mean feature vector of all neighboring nodes classified as $\mathcal{V}^m_{\text{some-known}}$.

3.2.3 Hop-wise Representation Enhancement. Despite the improvements in feature imputation for attribute-missing nodes achieved by DCFP and HNAI, the features of attribute-complete nodes remain static. Moreover, effective graph clustering often depends on aggregating multi-hop neighborhood information beyond a intrinsic features.

To address this, we propose Hop-wise Representation Enhancement (HRE), which captures multi-scale context by progressively performing message passing (MP) and concatenating features from multiple hops. At the k-th hop, node features are updated as:

$$\mathbf{H}^{(k)} = \hat{\mathbf{A}}\mathbf{H}^{(k-1)}, \tag{13}$$

where $\hat{\mathbf{A}}$ is the normalized adjacency matrix. After K hops, the final representation is formed by concatenating the features from all hops:

$$\mathbf{H}_E = [\mathbf{H}^{(0)}, \mathbf{H}^{(1)}, \ldots, \mathbf{H}^{(K)}]^\top \in \mathbb{R}^{n \times (K+1)d}. \tag{14}$$

Algorithm 1 Divide-Then-Rule Graph Completion (DTRGC)

Input: Feature matrix $\mathbf{H}$; Normalized adjacency matrix $\hat{\mathbf{A}}$; Attribute-missing nodes $\mathcal{V}^m$; Attribute-complete nodes $\mathcal{V}^c$; Maximum iterations $F_{\max}$, $I_{\max}$; Maximum propagation step K.

Output: Completed and enhanced feature matrix $\mathbf{H}_E \in \mathbb{R}^{n\times(K+1)d}$

/* Stage 1: DCFP */
for $t = 1$ to $F_{\max}$ **do**
  Update $\mathbf{H}^{(t+1)} \leftarrow \hat{\mathbf{A}}\mathbf{H}^{(t)}$
  Restore $\mathbf{H}_c^{(t+1)} \leftarrow \mathbf{H}_c^{(0)}$
  if t mod 40 == 0 **then**
    Update $\hat{\mathbf{A}}$ by Eq.(1)
  end if
end for
/* Stage 2: HNAI */
for $i = 1$ to $I_{\max}^{(H)}$ **do**
  Obtain $\mathcal{V}^m_{\text{all-known}}$, $\mathcal{V}^m_{\text{some-known}}$, $\mathcal{V}^m_{\text{all-unknown}}$ by Eq.(2)
  Update $\mathcal{V}^m_{\text{all-known}}$ by Eq.(4)
  for each node $v \in \mathcal{V}^m_{\text{some-known}}$ **do**
    Update $\mathcal{V}^m_{\text{some-known}}$ by Eq.(8)
    Update $\mathcal{V}^m_{\text{some-known}}$ and $\mathcal{V}^m$ by Eq.(7)
  end for
end for
for each node $v \in \mathcal{V}^m_{\text{all-unknown}}$ **do**
  Update $\mathcal{V}^m_{\text{all-unknown}}$ by Eq.(12)
end for
/* Stage 3: HRE */
for $k = 0$ to K **do**
  Update $\mathbf{H} \leftarrow \hat{\mathbf{A}}\mathbf{H}$
  Update $\mathbf{H}_E \leftarrow [\mathbf{H}_E; \mathbf{H}]$
end for
return $\mathbf{H}_E$

This formulation ensures that each node representation $\mathbf{s}_i \in \mathbb{R}^{(K+1)d}$ encodes hierarchical neighborhood information for downstream clustering.

3.3 Complexity Analysis

This section analyzes the computational complexity of the three main components of the proposed DTRGC framework: DCFP, HNAI, and HRE. The total complexity is the sum of the individual components:

$$O\Big(K_1|E|d + \frac{K_1}{T}ncdi + K_2ncdi + K_2nd_{\text{avg}} + K_3|E|d + K_3nd\Big), \quad (15)$$

where, K_1 is the number of propagation steps in DCFP, $|E|$ is the number of edges, and d is the feature dimension of the node attribute matrix $\mathbf{H}$, T is the number of iterations for adjusting the adjacency matrix in DCFP, n is the number of nodes, c is the number of clusters, and i is the number of k-means iterations, d_{avg} is the average degree of nodes, and K_2, K_3 are the number of iterations for HNAI and HRE, respectively.

This total complexity can be simplified to $O(n + |E|)$, indicating that the proposed DTRGC exhibits a linear relationship with both the number of nodes and the number of edges. Detailed complexity derivations can be found in the supplementary materials.

4 Experiments

This section describes the experimental setup and evaluates DTRGC by answering the following questions:

- **Q1:** How does the performance of different DGC improve with integrating DTRGC under conditions of missing attributes?
- **Q2:** What is the contribution of each component to clustering performance?
- **Q3:** How does DTRGC perform in comparison to node classification baselines on attribute-missing graphs?
- **Q4:** How does the hierarchical processing in DTRGC alleviate issues related to nodes with all unknown neighbors being interconnected?
- **Q5:** How does DTRGC improve the clustering friendliness of attribute-missing nodes?

Q1–Q4 are addressed in the main text, while Q5 is further analyzed in the supplementary material.

4.1 Experimental Settings

Datasets. To facilitate a comprehensive comparison of the proposed model, six benchmark datasets are selected, including: (1) citation graphs: Cora, Citeseer, and Pubmed; (2) co-purchase graph: Amap; and (3) co-authorship graphs: Co.CS and Co.Physics.

Compared Methods. To evaluate the imputation effectiveness of DTRGC, several state-of-the-art DGC methods are selected, and their clustering performance is compared in two scenarios: (1) the original clustering performance on attribute-missing graphs; and (2) the clustering performance after DTRGC imputation. This comparison directly assesses the impact of DTRGC on improving clustering performance. The methods included in this comparison are GDCL [56], AGCN [23], AGC-DRR [4], HSAN [16], CCGC [41], and AMGC [28].

Experiment Setup. To ensure a fair comparison, 10 experimental iterations are conducted under identical conditions and compute the average results. All experiments run on hardware with a 24GB RTX 3090 GPU and 64GB RAM. The comparison experiments are performed with a 0.6 missing rate, meaning 40% of node attributes in the original graph are randomly retained, while all attributes of the remaining 60% of nodes are removed and set as zero vectors. Further details on the experimental setup follow the settings in AMGC [28].

4.2 Clustering Performance Comparison (Q1)

The comparison of clustering performance before and after imputation is shown in Table 1, which presents the experimental results of combining DTRGC with various graph clustering methods across six datasets. The following observations can be made from these results:

- Across all datasets, incorporating DTRGC consistently leads to significant improvements in clustering performance metrics. For instance, on the Cora dataset, the ACC of the AMGC model increased from 66.65 ± 2.04 to 70.66 ± 1.25, showing an absolute improvement of over 4%.
- For certain DGC methods that exhibit nearly unacceptable performance under missing attribute scenarios, such as GDCL,

Table 1: The clustering performance on six benchmark datasets (mean±std). The best and runner-up results are highlighted with bold and underline, respectively. 'OOM' means the out-of-memory failure.

Dataset	Metric	DGC (No Completion)						DGC + DTRGC (Pre-Completion)					
		GDCL IJCAI21	AGCN MM21	AGC-DRR IJCAI22	HSAN AAAI23	CCGC AAAI23	AMGC AAAI24	GDCL IJCAI21	AGCN MM21	AGC-DRR IJCAI22	HSAN AAAI23	CCGC AAAI23	AMGC AAAI24
Cora	ACC	24.76±1.84	39.88±3.18	43.26±7.09	57.94±1.27	37.93±2.68	**66.65±2.04**	54.23±1.32	57.81±2.24	62.27±2.46	63.81±1.29	54.29±1.54	**70.66±1.25**
	NMI	4.74±2.21	19.16±1.43	23.26±8.51	42.01±1.24	22.37±3.03	**47.99±1.67**	34.21±0.74	35.59±2.23	38.24±3.57	44.12±0.91	37.43±0.31	**56.29±1.14**
	ARI	0.74±1.04	14.09±3.75	16.23±8.41	33.14±1.78	11.45±2.81	**43.40±1.90**	27.41±1.32	30.21±1.44	34.54±4.29	38.75±1.92	32.68±1.44	**46.51±1.46**
	F1	7.82±2.16	33.96±2.64	31.09±8.21	58.77±0.89	36.91±4.12	**61.02±2.38**	35.46±1.22	37.21±2.88	44.51±4.41	60.24±1.22	55.43±0.47	**66.31±1.11**
Citeseer	ACC	27.39±2.19	42.22±2.78	30.95±4.26	44.22±0.52	39.63±1.95	**60.92±2.01**	54.26±1.07	56.13±1.32	51.17±0.84	60.34±1.77	55.64±2.88	**64.77±1.31**
	NMI	7.53±2.38	19.01±1.74	13.26±3.41	22.29±1.39	17.13±1.34	**32.93±1.71**	21.45±1.74	27.17±2.21	24.97±2.33	33.27±2.47	25.31±0.75	**37.44±1.24**
	ARI	2.25±1.08	13.31±2.17	2.35±3.43	13.32±1.08	11.83±2.34	**33.73±2.25**	21.45±2.23	27.88±3.45	24.31±1.87	34.45±1.47	31.471±1.51	**38.58±1.56**
	F1	12.16±4.02	37.22±1.67	29.10±5.26	42.18±2.54	38.88±2.54	**57.33±2.05**	38.48±2.87	52.91±1.33	44.31±4.46	58.91±2.14	54.74±2.31	**60.18±1.32**
Amap	ACC	43.34±3.15	43.73±2.81	61.89±5.96	62.36±2.61	51.20±2.25	**67.56±3.01**	64.78±2.88	62.61±3.74	72.31±2.27	71.86±2.34	67.74±2.41	**75.65±2.50**
	NMI	30.94±6.37	34.63±4.72	55.33±5.32	51.42±1.26	41.13±2.41	**59.81±1.58**	59.27±4.46	60.01±4.79	63.94±4.37	62.57±3.46	57.61±2.48	**66.94±2.37**
	ARI	22.42±4.33	22.93±4.97	41.43±5.18	41.09±2.43	30.74±1.06	**49.22±2.75**	48.15±5.78	45.17±3.13	52.23±5.33	54.56±3.15	49.79±1.78	**57.14±3.34**
	F1	24.77±3.87	32.74±2.51	**61.35±7.40**	55.06±2.40	46.17±4.38	59.49±3.43	58.15±2.78	64.74±2.45	67.62±5.13	62.48±4.84	59.41±3.41	**69.66±2.47**
PubMed	ACC	47.00±0.39	41.85±2.28	60.71±1.72	OOM	42.70±1.49	**64.56±1.50**	63.48±0.71	58.12±2.12	66.71±1.21	OOM	59.15±1.24	**67.81±2.12**
	NMI	10.84±0.49	0.93±1.08	16.26±2.14		2.43±1.75	**24.58±2.21**	18.48±0.24	12.61±0.74	27.61±1.87		14.91±1.69	**30.07±2.13**
	ARI	7.39±0.27	1.37±1.18	17.35±2.44		1.24±0.87	**24.19±2.39**	16.57±0.24	14.71±1.31	23.74±1.71		16.77±0.47	**29.24±2.65**
	F1	28.36±10.56	36.05±0.79	59.80±2.43		34.28±3.16	**64.52±1.26**	54.78±4.31	60.47±0.84	65.48±2.13		59.41±1.69	**67.30±1.94**
Co.CS	ACC	40.18±1.63	52.13±5.88	59.08±2.26	OOM	64.88±1.51	**72.61±1.08**	59.24±1.44	61.07±4.23	64.84±0.78	OOM	69.48±1.57	**74.44±0.94**
	NMI	41.67±1.29	49.51±5.30	64.16±1.97		63.21±0.82	**73.91±0.39**	52.67±1.43	57.81±1.57	67.75±1.61		68.15±0.91	**75.27±0.46**
	ARI	15.32±1.68	41.44±7.43	49.27±2.86		55.08±2.22	**64.62±0.66**	44.59±2.04	52.59±3.32	58.61±2.74		64.59±0.77	**69.31±0.34**
	F1	3.62±2.78	25.02±5.54	45.09±1.41		54.17±2.76	**68.34±1.88**	44.33±2.41	54.61±1.67	59.47±1.81		66.87±1.71	**71.03±2.12**
Co.Physics	ACC	OOM	63.64±4.06	OOM	OOM	OOM	**77.68±3.78**	OOM	66.71±3.94	OOM	OOM	OOM	**80.67±1.32**
	NMI		34.98±7.68				**62.77±1.46**		54.31±6.41				**65.17±1.04**
	ARI		43.94±6.91				**69.00±6.25**		54.11±4.79				**72.61±3.21**
	F1		43.19±6.61				**67.58±2.68**		54.52±6.15				**69.31±2.41**

incorporating DTRGC significantly boosts their clustering performance to an acceptable level. For example, on the PubMed dataset, the ACC of GDCL improved from 47.00 ± 0.39 to 63.48 ± 0.71.

- The occurrence of out-of-memory (OOM) failures remains consistent before and after applying DTRGC, indicating that DTRGC does not introduce additional memory overhead that leads to OOM issues.

4.3 T-SNE Visualization (Q1)

To visually assess the effectiveness of DTRGC, 2D t-distributed Stochastic Neighbor Embedding (t-SNE) [33] is employed to compare the clustering performance of six baseline algorithms before and after imputation. As shown in Fig.3, compared to their original versions without DTRGC, the DGC methods with DTRGC imputation exhibit significantly higher intra-cluster compactness and more pronounced inter-cluster separation.

4.4 Ablation Study (Q2)

We progressively remove the three stages of DTRGC to create different variants, aiming to evaluate the independent contribution of each component. It is important to note that DTRGC is not a complete DGC method but rather a plug-and-play imputation module. Therefore, in the ablation experiments, we choose AMGC, which shows the best performance when combined with DTRGC, as the baseline model.

As summarized in Table 2, each component of the proposed model significantly contributes to the enhancement of clustering

Table 2: Ablation study results on four benchmark datasets, reporting clustering performance metrics (mean ± std). The best results are highlighted in bold.

Datasets	Method	ACC	NMI	ARI	F1
Cora	Base	66.65±2.04	47.99±1.67	43.40±1.90	61.02±2.38
	w/o DCFP	67.72±1.75	51.71±1.12	44.34±1.81	63.07±2.07
	w/o HNAI	67.84±1.48	49.31±1.04	44.52±1.61	62.91±1.91
	w/o HRE	69.75±1.32	55.48±1.63	45.97±1.77	65.81±1.41
	w/o DCFP and HNAI	67.24±1.51	48.57±1.24	43.84±1.43	62.44±2.37
	w/o DCFP and HRE	67.79±1.44	49.32±1.33	43.91±1.54	62.77±1.43
	w/o HNAI and HRE	67.07±1.43	48.83±2.34	43.84±1.61	62.33±1.49
	DTRGC	**70.66±1.25**	**56.29±1.14**	**46.51±1.46**	**66.31±1.11**
Citeseer	Base	60.92±2.01	32.93±1.71	33.20±2.25	57.33±2.05
	w/o DCFP	62.45±1.72	33.80±1.58	33.84±1.97	58.17±1.86
	w/o HNAI	62.90±1.53	34.75±1.39	35.32±1.76	59.72±1.67
	w/o HRE	63.41±1.45	36.54±1.47	37.13±1.69	59.46±1.62
	w/o DCFP and HNAI	61.98±1.58	33.59±1.55	34.04±1.54	57.92±1.73
	w/o DCFP and HRE	62.95±1.50	34.32±1.43	34.70±1.61	58.50±1.75
	w/o HNAI and HRE	62.42±1.51	33.55±1.44	34.54±1.59	59.12±1.68
	DTRGC	**64.70±1.31**	**37.44±1.24**	**38.58±1.56**	**60.18±1.32**
Amap	Base	67.56±3.01	59.81±1.58	49.22±2.75	59.49±3.43
	w/o DCFP	70.45±2.55	62.20±1.42	52.70±2.38	63.05±2.95
	w/o HNAI	71.32±2.74	62.45±1.37	53.12±2.51	63.58±3.08
	w/o HRE	74.11±2.62	65.15±1.50	55.80±2.63	67.33±3.22
	w/o DCFP and HNAI	69.50±2.65	60.78±1.49	50.32±2.49	61.18±3.01
	w/o DCFP and HRE	70.10±2.59	61.35±1.43	51.50±2.42	62.13±2.97
	w/o HNAI and HRE	71.21±2.60	62.02±1.48	52.60±2.54	62.60±2.54
	DTRGC	**75.65±2.50**	**66.94±2.37**	**57.14±3.34**	**69.66±2.47**
Pubmed	Base	64.56±1.50	24.58±2.21	24.19±2.39	64.52±1.26
	w/o DCFP	66.78±1.42	26.35±2.01	25.20±2.26	65.90±1.35
	w/o HNAI	66.12±1.34	27.12±1.95	25.85±2.31	65.35±1.41
	w/o HRE	66.85±1.29	28.65±2.03	28.14±2.24	66.74±1.38
	w/o DCFP and HNAI	65.20±1.47	25.90±2.10	24.75±2.28	65.11±1.31
	w/o DCFP and HRE	65.65±1.38	26.22±2.05	24.87±2.30	65.75±1.33
	w/o HNAI and HRE	65.44±1.31	26.80±2.08	25.08±2.27	66.10±1.36
	DTRGC	**67.81±2.12**	**30.07±2.13**	**29.24±2.65**	**67.30±1.94**

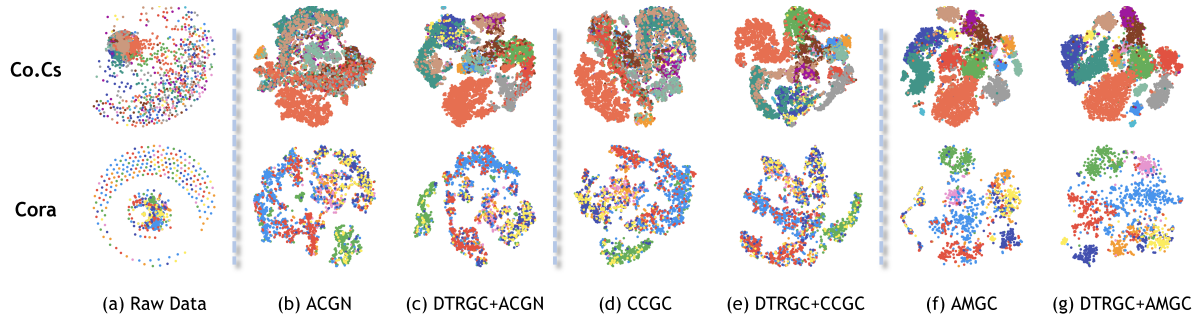

Figure 3: T-SNE visualization of node embeddings.

performance. Specifically, considering the accuracy (ACC) as an example, the improvements introduced by DCFP, HNAI, and HRE across the four datasets were observed as follows: Cora: 0.42%, 1.14%, and 0.59%; Citeseer: 1.50%, 2.03%, and 1.06%; Amap: 3.65%, 2.54%, and 1.94%; Pubmed: 0.88%, 1.09%, and 0.64%, respectively. A consistent pattern of improvement is also reflected across other evaluation metrics.

Additionally, when DCFP and HNAI were jointly employed, the resulting performance gains were significantly greater compared to the individual contributions of these two components, yielding improvements of 3.10%, 4.09%, 6.55%, and 3.55% on the Cora, Citeseer, Amap, and Pubmed datasets, respectively. These findings suggest that: (1) The hierarchical imputation provided by HNAI demonstrates a synergistic effect when integrated with DCFP. (2) The enhancement contributed by HRE appears largely independent of DCFP and HNAI, which suggests that its capability in improving representation quality has broader applicability.

4.5 Node Classification Comparison (Q3)

As a plug-and-play imputation solution, DTRGC not only performs well in clustering on attribute-missing graphs but is also applicable to a classic learning task on attribute-missing graphs—semi-supervised node classification. The experimental setup and comparison methods follow the current state-of-the-art node classification approach for attribute-missing graphs, PCFI [32]. Specifically, under a missing rate of 0.995, we compare the node classification performance of DTRGC with GCNMF [26], PaGNN [7] and FP [24]. For plug-and-play imputation methods, we use vanilla GCN for the subsequent node classification tasks.

Table 3 presents the experimental results under a 0.995 missing rate scenario. It is evident that both DTRGC and PCFI outperform other methods across all datasets. Notably, DTRGC surpasses PCFI on the Cora, Computers, and ogbn-Arxiv datasets, achieving an accuracy of 76.12% on Cora, 79.43% on Computers, and 69.24% on ogbn-Arxiv. Despite being initially designed for clustering, DTRGC demonstrates competitive performance in the semi-supervised node classification, highlighting its robustness and strong generalization capability across a variety of graph learning scenarios.

4.6 Effectiveness of Hierarchical Processing (Q4)

To validate the effectiveness of the HNAI module within DTRGC, a set of experiments are designed to track the evolution of three types of nodes across different datasets. This aims to analyze their transformation over multiple iterations. As shown in Fig. 4, the trend in the number of three types of nodes is anylised over multiple iterations across six datasets: Cora, PubMed, CiteSeer, CS, Amap, and Physics. The experimental results indicate that the HNAI module within DTRGC significantly reduces the number of "nodes with partially known neighbors" and "nodes with all unknown neighbors", especially in the initial iterations, where the counts of these nodes drop sharply. Specifically, HNAI first processes "nodes with all known neighbors" and "nodes with partially known neighbors," using them as anchors for feature recovery and then gradually leveraging the recovered information to affect other attribute-missing nodes. As iterations progress, subgraphs composed of interconnected "nodes with all unknown neighbors" gradually gain reliable information from surrounding nodes, reducing the negative impact of indiscriminate propagation on clustering.

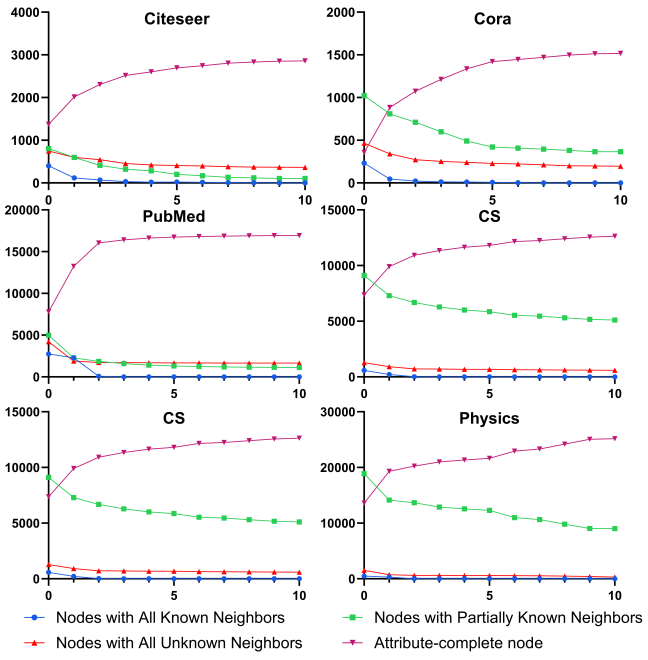

Figure 4: The number of three node types over different iterations.

Table 3: Comparison of classification accuracy (acc) across benchmark datasets for different imputation methods in semi-supervised node classification tasks with a missing rate of 0.995 (mean±std). The best results are highlighted in bold.

Dataset	GCNMF	PaGNN	FP	PCFI	DTRGC
Cora	29.20±0.71	30.55±8.85	72.84±2.85	75.49±2.10	**76.12±2.03**
Citeseer	24.50±1.52	25.69±3.98	59.76±2.47	**66.18±2.75**	65.34±1.64
PubMed	40.19±0.95	50.82±4.61	72.69±2.66	**74.66±2.26**	73.31±2.47
Photo	26.82±6.33	66.91±3.99	86.57±1.50	**87.70±1.29**	86.94±1.13
Computers	30.59±9.81	56.50±3.29	77.45±1.59	79.25±1.19	**79.43±1.45**
ogbn-Arxiv	OOM	OOM	68.23±0.27	68.72±0.28	**69.24±0.47**

5 Conclusion and Future Work

This paper proposes a framework, termed DTRGC, to address challenges in clustering attribute-missing graphs. Unlike existing imputation methods that often overlook varying levels of neighborhood information availability, DTRGC prioritizes nodes with richer neighborhood information, allowing them to serve as reliable anchors for subsequent imputation of more challenging nodes. Experimental results on six widely used graph datasets confirm that DTRGC significantly enhances the clustering performance of attribute-missing graphs across various DGC methods. As a direction for future research, we intend to develop a parametric extension of DTRGC, aiming to further improve its adaptability, model complexity, and performance across a broader range of heterogeneous graph datasets and real-world applications.

References

[1] Wei Ai, Yuntao Shou, Tao Meng, Nan Yin, and Keqin Li. 2023. Der-gcn: Dialogue and event relation-aware graph convolutional neural network for multimodal dialogue emotion recognition. *arXiv preprint arXiv:2312.10579* (2023).

[2] Wendong Bi, Lun Du, Qiang Fu, Yanlin Wang, Shi Han, and Dongmei Zhang. 2024. Make Heterophilic Graphs Better Fit GNN: A Graph Rewiring Approach. *IEEE Transactions on Knowledge and Data Engineering* 36, 12 (2024), 8744–8757. doi:10.1109/TKDE.2024.3441766

[3] Xu Chen, Siheng Chen, Jiangchao Yao, Huangjie Zheng, Ya Zhang, and Ivor W Tsang. 2020. Learning on attribute-missing graphs. *IEEE transactions on pattern analysis and machine intelligence* 44, 2 (2020), 740–757.

[4] Lei Gong, Sihang Zhou, Wenxuan Tu, and Xinwang Liu. 2022. Attributed Graph Clustering with Dual Redundancy Reduction.. In *IJCAI*. 3015–3021.

[5] David Haynes, Steven Corns, and Ganesh Kumar Venayagamoorthy. 2012. An exponential moving average algorithm. In *2012 IEEE Congress on Evolutionary Computation*. IEEE, 1–8.

[6] Cuiying Huo, Di Jin, Yawen Li, Dongxiao He, Yu-Bin Yang, and Lingfei Wu. 2023. T2-gnn: Graph neural networks for graphs with incomplete features and structure via teacher-student distillation. In *Proceedings of the AAAI Conference on Artificial Intelligence*, Vol. 37. 4339–4346.

[7] Bo Jiang and Ziyan Zhang. 2020. Incomplete graph representation and learning via partial graph neural networks. *arXiv preprint arXiv:2003.10130* (2020).

[8] Di Jin, Cuiying Huo, Chundong Liang, and Liang Yang. 2021. Heterogeneous Graph Neural Network via Attribute Completion. In *Proceedings of the Web Conference 2021 (WWW '21)*. 391–400.

[9] Di Jin, Rui Wang, Tao Wang, Dongxiao He, Weiping Ding, Yuxiao Huang, Longbiao Wang, and Witold Pedrycz. 2022. Amer: A new attribute-missing network embedding approach. *IEEE Transactions on Cybernetics* 53, 7 (2022), 4306–4319.

[10] Wei Ju, Siyu Yi, Yifan Wang, Zhiping Xiao, Zhengyang Mao, Hourun Li, Yiyang Gu, Yifang Qin, Nan Yin, Senzhang Wang, et al. 2024. A survey of graph neural networks in real world: Imbalance, noise, privacy and ood challenges. *arXiv preprint arXiv:2403.04468* (2024).

[11] Thomas N Kipf and Max Welling. 2017. Semi-supervised classification with graph convolutional networks. *5th International Conference on Learning Representations (ICLR)* (2017).

[12] Mengran Li, Yong Zhang, Wei Zhang, Shiyu Zhao, Xinglin Piao, and Baocai Yin. 2022. Csat: Contrastive Sampling-Aggregating Transformer for Attribute-Missing Graph Learning. *Available at SSRN 4278482* (2022).

[13] Fan Liu, Zhiyong Cheng, Lei Zhu, Chenghao Liu, and Liqiang Nie. 2022. An Attribute-Aware Attentive GCN Model for Attribute Missing in Recommendation. *IEEE Transactions on Knowledge and Data Engineering* 34, 9 (2022), 4077–4088. doi:10.1109/TKDE.2020.3040772

[14] Yue Liu, Wenxuan Tu, Sihang Zhou, Xinwang Liu, Linxuan Song, Xihong Yang, and En Zhu. 2022. Deep graph clustering via dual correlation reduction. In *Proceedings of the AAAI conference on artificial intelligence*, Vol. 36. 7603–7611.

[15] Yue Liu, Xihong Yang, Sihang Zhou, Xinwang Liu, Siwei Wang, Ke Liang, Wenxuan Tu, and Liang Li. 2023. Simple contrastive graph clustering. *IEEE Transactions on Neural Networks and Learning Systems* (2023).

[16] Yue Liu, Xihong Yang, Sihang Zhou, Xinwang Liu, Zhen Wang, Ke Liang, Wenxuan Tu, Liang Li, Jingcan Duan, and Cancan Chen. 2023. Hard sample aware network for contrastive deep graph clustering. In *Proceedings of the AAAI conference on artificial intelligence*, Vol. 37. 8914–8922.

[17] Tao Meng, Yuntao Shou, Wei Ai, Nan Yin, and Keqin Li. 2024. Deep imbalanced learning for multimodal emotion recognition in conversations. *IEEE Transactions on Artificial Intelligence* (2024).

[18] Nairouz Mrabah, Mohamed Bouguessa, Mohamed Fawzi Touati, and Riadh Ksantini. 2023. Rethinking Graph Auto-Encoder Models for Attributed Graph Clustering. *IEEE Transactions on Knowledge and Data Engineering* 35, 9 (2023), 9037–9053. doi:10.1109/TKDE.2022.3220948

[19] Shirui Pan, Ruiqi Hu, Sai-fu Fung, Guodong Long, Jing Jiang, and Chengqi Zhang. 2019. Learning graph embedding with adversarial training methods. *IEEE transactions on cybernetics* 50, 6 (2019), 2475–2487.

[20] Jinhui Pang, Zixuan Wang, Jiliang Tang, Mingyan Xiao, and Nan Yin. 2023. Sagda: Spectral augmentation for graph domain adaptation. In *Proceedings of the 31st ACM International Conference on Multimedia*. 309–318.

[21] Namyong Park, Ryan Rossi, Eunyee Koh, Iftikhar Ahamath Burhanuddin, Sungchul Kim, Fan Du, Nesreen Ahmed, and Christos Faloutsos. 2022. CGC: Contrastive Graph Clustering for Community Detection and Tracking. In *Proceedings of the Web Conference 2022 (WWW '22)*. 1115–1126.

[22] Xin Peng, Jieren Cheng, Xiangyan Tang, Jingxin Liu, and Jiahua Wu. 2023. Dual contrastive learning network for graph clustering. *IEEE Transactions on Neural Networks and Learning Systems* (2023).

[23] Zhihao Peng, Hui Liu, Yuheng Jia, and Junhui Hou. 2021. Attention-driven graph clustering network. In *Proceedings of the 29th ACM international conference on multimedia*. 935–943.

[24] Emanuele Rossi, Henry Kenlay, Maria I Gorinova, Benjamin Paul Chamberlain, Xiaowen Dong, and Michael M Bronstein. 2022. On the unreasonable effectiveness of feature propagation in learning on graphs with missing node features. In *Learning on graphs conference*. PMLR, 11–1.

[25] Yuntao Shou, Tao Meng, Wei Ai, Nan Yin, and Keqin Li. 2023. Adversarial representation with intra-modal and inter-modal graph contrastive learning for multimodal emotion recognition. *arXiv preprint arXiv:2312.16778* (2023).

[26] Hibiki Taguchi, Xin Liu, and Tsuyoshi Murata. 2021. Graph convolutional networks for graphs containing missing features. *Future Generation Computer Systems* 117 (2021), 155–168.

[27] Zhiqiang Tao, Hongfu Liu, Jun Li, Zhaowen Wang, and Yun Fu. 2019. Adversarial graph embedding for ensemble clustering. In *International Joint Conferences on Artificial Intelligence Organization*.

[28] Wenxuan Tu, Renxiang Guan, Sihang Zhou, Chuan Ma, Xin Peng, Zhiping Cai, Zhe Liu, Jieren Cheng, and Xinwang Liu. 2024. Attribute-missing graph clustering network. In *Proceedings of the AAAI Conference on Artificial Intelligence*, Vol. 38. 15392–15401.

[29] Wenxuan Tu, Sihang Zhou, Xinwang Liu, Chunpeng Ge, Zhiping Cai, and Yue Liu. 2023. Hierarchically contrastive hard sample mining for graph self-supervised pretraining. *IEEE Transactions on Neural Networks and Learning Systems* (2023).

[30] Wenxuan Tu, Sihang Zhou, Xinwang Liu, Xifeng Guo, Zhiping Cai, En Zhu, and Jieren Cheng. 2021. Deep fusion clustering network. In *Proceedings of the AAAI conference on artificial intelligence*, Vol. 35. 9978–9987.

[31] Wenxuan Tu, Sihang Zhou, Xinwang Liu, Yue Liu, Zhiping Cai, En Zhu, Changwang Zhang, and Jieren Cheng. 2022. Initializing Then Refining: A Simple Graph Attribute Imputation Network.. In *IJCAI*. 3494–3500.

[32] Daeho Um, Jiwoong Park, Seulki Park, and Jin Young Choi. 2023. Confidence-based feature imputation for graphs with partially known features. *The Eleventh International Conference on Learning Representations (ICLR)* (2023).

[33] Laurens Van der Maaten and Geoffrey Hinton. 2008. Visualizing data using t-SNE. *Journal of machine learning research* 9, 11 (2008).

[34] Eline Van Geert and Johan Wagemans. 2024. Prägnanz in visual perception. *Psychonomic Bulletin & Review* 31, 2 (2024), 541–567.

[35] Chun Wang, Shirui Pan, Ruiqi Hu, Guodong Long, Jing Jiang, and Chengqi Zhang. 2019. Attributed graph clustering: A deep attentional embedding approach. *arXiv preprint arXiv:1906.06532* (2019).

[36] Yaohua Wang, Yaobin Zhang, Fangyi Zhang, Ming Lin, YuQi Zhang, Senzhang Wang, and Xiuyu Sun. 2022. Ada-nets: Face clustering via adaptive neighbour discovery in the structure space. *arXiv preprint arXiv:2202.03800* (2022).

[37] Jun Xia, Haitao Lin, Yongjie Xu, Cheng Tan, Lirong Wu, Siyuan Li, and Stan Z. Li. 2024. GNN Cleaner: Label Cleaner for Graph Structured Data. *IEEE Transactions on Knowledge and Data Engineering* 36, 2 (2024), 640–651. doi:10.1109/TKDE.2023.3288002

[38] Wei Xia, Qianqian Wang, Quanxue Gao, Ming Yang, and Xinbo Gao. 2022. Self-consistent contrastive attributed graph clustering with pseudo-label prompt. *IEEE Transactions on Multimedia* 25 (2022), 6665–6677.

[39] Zhu Xiaojin and Ghahramani Zoubin. 2002. Learning from labeled and unlabeled data with label propagation. In *Tech. Rep., Technical Report CMU-CALD-02–107*. Carnegie Mellon University.

[40] Hansheng Xue, Vijini Mallawaarachchi, Yujia Zhang, Vaibhav Rajan, and Yu Lin. 2022. RepBin: constraint-based graph representation learning for metagenomic binning. In *Proceedings of the AAAI Conference on Artificial Intelligence*, Vol. 36. 4637–4645.

[41] Xihong Yang, Yue Liu, Sihang Zhou, Siwei Wang, Wenxuan Tu, Qun Zheng, Xinwang Liu, Liming Fang, and En Zhu. 2023. Cluster-guided contrastive graph clustering network. In *Proceedings of the AAAI conference on artificial intelligence*, Vol. 37. 10834–10842.

[42] Nan Yin, Fuli Feng, Zhigang Luo, Xiang Zhang, Wenjie Wang, Xiao Luo, Chong Chen, and Xian-Sheng Hua. 2022. Dynamic hypergraph convolutional network. In *2022 IEEE 38th International Conference on Data Engineering (ICDE)*. IEEE, 1621–1634.

[43] Nan Yin and Zhigang Luo. 2022. Generic structure extraction with bi-level optimization for graph structure learning. *Entropy* 24, 9 (2022), 1228.

[44] Nan Yin, Li Shen, Chong Chen, Xian-Sheng Hua, and Xiao Luo. [n. d.]. SPORT: A Subgraph Perspective on Graph Classification with Label Noise. *ACM Transactions on Knowledge Discovery from Data* ([n. d.]).

[45] Nan Yin, Li Shen, Baopu Li, Mengzhu Wang, Xiao Luo, Chong Chen, Zhigang Luo, and Xian-Sheng Hua. 2022. Deal: An unsupervised domain adaptive framework for graph-level classification. In *Proceedings of the 30th ACM International Conference on Multimedia*. 3470–3479.

[46] Nan Yin, Li Shen, Mengzhu Wang, Long Lan, Zeyu Ma, Chong Chen, Xian-Sheng Hua, and Xiao Luo. 2023. Coco: A coupled contrastive framework for unsupervised domain adaptive graph classification. In *International Conference on Machine Learning*. PMLR, 40040–40053.

[47] Nan Yin, Li Shen, Mengzhu Wang, Xiao Luo, Zhigang Luo, and Dacheng Tao. 2023. Omg: towards effective graph classification against label noise. *IEEE Transactions on Knowledge and Data Engineering* (2023).

[48] Nan Yin, Li Shen, Huan Xiong, Bin Gu, Chong Chen, Xian-Sheng Hua, Siwei Liu, and Xiao Luo. 2023. Messages are never propagated alone: Collaborative hypergraph neural network for time-series forecasting. *IEEE Transactions on Pattern Analysis and Machine Intelligence* (2023).

[49] Nan Yin, Mengzhu Wan, Li Shen, Hitesh Laxmichand Patel, Baopu Li, Bin Gu, and Huan Xiong. 2024. Continuous Spiking Graph Neural Networks. *arXiv preprint arXiv:2404.01897* (2024).

[50] Nan Yin, Mengzhu Wang, Zhenghan Chen, Giulia De Masi, Huan Xiong, and Bin Gu. 2024. Dynamic spiking graph neural networks. In *Proceedings of the AAAI Conference on Artificial Intelligence*, Vol. 38. 16495–16503.

[51] Nan Yin, Mengzhu Wang, Zhenghan Chen, Li Shen, Huan Xiong, Bin Gu, and Xiao Luo. 2023. DREAM: Dual Structured Exploration with Mixup for Open-set Graph Domain Adaption. In *The Twelfth International Conference on Learning Representations*.

[52] Jaemin Yoo, Hyunsik Jeon, Jinhong Jung, and U Kang. 2022. Accurate node feature estimation with structured variational graph autoencoder. In *Proceedings of the 28th ACM SIGKDD Conference on Knowledge Discovery and Data Mining*. 2336–2346.

[53] Bowen Zhang, Xianghua Fu, Daijun Ding, Hu Huang, Genan Dai, Nan Yin, Yangyang Li, and Liwen Jing. 2023. Investigating chain-of-thought with chatgpt for stance detection on social media. *arXiv preprint arXiv:2304.03087* (2023).

[54] Hongyuan Zhang, Pei Li, Rui Zhang, and Xuelong Li. 2022. Embedding graph auto-encoder for graph clustering. *IEEE Transactions on Neural Networks and Learning Systems* 34, 11 (2022), 9352–9362.

[55] Xiaotong Zhang, Han Liu, Qimai Li, Xiao-Ming Wu, and Xianchao Zhang. 2023. Adaptive Graph Convolution Methods for Attributed Graph Clustering. *IEEE Transactions on Knowledge and Data Engineering* 35, 12 (2023), 12384–12399. doi:10.1109/TKDE.2023.3278721

[56] Han Zhao, Xu Yang, Zhenru Wang, Erkun Yang, and Cheng Deng. 2021. Graph Debiased Contrastive Learning with Joint Representation Clustering.. In *IJCAI*. 3434–3440.

[57] Pengfei Zhu, Xinjie Yao, Yu Wang, Meng Cao, Binyuan Hui, Shuai Zhao, and Qinghua Hu. 2022. Latent heterogeneous graph network for incomplete multi-view learning. *IEEE Transactions on Multimedia* 25 (2022), 3033–3045.